

## Numerical analysis of FGM plates with variable thickness subjected to thermal buckling

Otbi Bouguenina<sup>1</sup>, Khalil Belakhdar<sup>\*2</sup>,  
Abdelouahed Tounsi<sup>3</sup> and El Abbas Adda Bedia<sup>3</sup>

<sup>1</sup> Department of Civil Engineering and Hydraulics, University of Saida,  
BP 138 Cité Ennacer, 20000 Saida, Algeria

<sup>2</sup> Department of Science and Technology, University Centre of Tamanrasset,  
BP 10034 Sersouf, Tamanrasset, Algeria

<sup>3</sup> Laboratory of Materials and Hydrology, University of Sidi Bel Abbès,  
BP 89 Cité Ben Mhidi, 22000 Sidi Bel Abbès, Algeria

(Received December 12, 2014, Revised February 04, 2015, Accepted February 09, 2015)

**Abstract.** A numerical solution using finite difference method to evaluate the thermal buckling of simply supported FGM plate with variable thickness is presented in this research. First, the governing differential equation of thermal stability under uniform temperature through the plate thickness is derived. Then, the governing equation has been solved using finite difference method. After validating the presented numerical method with the analytical solution, the finite difference formulation has been extended in order to include variable thickness. The accuracy of the finite difference method for variable thickness plate has been also compared with the literature where a good agreement has been found. Furthermore, a parametric study has been conducted to analyze the effect of material and geometric parameters on the thermal buckling resistance of the FGM plates. It was found that the thickness variation affects isotropic plates a bit more than FGM plates.

**Keywords:** FGM plate; thermal buckling; stability analysis; finite difference; numerical method

---

### 1. Introduction

Functionally graded materials (FGM) are considered as composite materials with smoothly varying properties through the thickness. The smoothness can be realized by gradually varying the volume fraction of the constituent materials. Usually, FGM are composed of metal and ceramic, where the metal has a high mechanical strength compared to ceramic material, while the ceramic material is characterized by its excellent resistance in high temperature environment due to its low thermal conductivity. Nowadays, FGM are used in many engineering and industrial domains, aircraft, space vehicles, etc., because they have excellent mechanical properties under high temperature environment.

Because of the advantages of FGM, a number of researches have been carried out to investigate

---

\*Corresponding author, Ph.D., E-mail: [be.khalil@gmail.com](mailto:be.khalil@gmail.com)

the behavior of FGM under thermal environment. Many different theories and solutions are suggested in the literature (Noseir and Reddy 1992, Rohit and Maiti 2012, Koohkan *et al.* 2010, Mohammadi *et al.* 2010, Fekrar *et al.* 2013, Praveen and Reddy 1998). Hiroyuki (2009) investigated the thermal and mechanical analysis of FGM plates based on two-dimensional higher-order deformation theory through using power series expansion for the evaluation of displacements and stresses. Bouazza *et al.* (2009) analyzed thermal buckling behavior of a sigmoid distribution of FGM plates under uniform, linear, and sinusoidal temperature rise across the thickness. They used the first order shear deformation theory and the results are compared to those of classical plate theory. Zenkour and Mashat (2010) proposed a sinusoidal shear deformation plate theory (SPT) for analyzing thermal buckling of FGM plates. They compared the results with those obtained by using HPT, FPT and CPT where they found that their results are very close to those of HPT. Raki *et al.* (2012) presented a closed-form solution based on higher order shear deformation theory to investigate the critical buckling temperature. A uniform and gradient temperature through the thickness is considered. The results are compared with those obtained by finite element method. Javaheri and Eslami (2002a, b) carried out a mechanical and thermal buckling analysis of FGM plates based on the classical plate theory; furthermore, they studied also the thermal buckling of FGM plates using higher order shear deformation theory (2002c). Lanhe (2004) conducted a research work to study the thermal buckling of moderately thick rectangular FGPs based on the first order shear deformation theory.

It should be mentioned that plates with constant thickness have been extensively studied. Even so, the variable thickness plates have also attracted the attention of designers and researchers. Such modification in shape can better enhance the smoothness of the stress distribution through decreasing the geometrical discontinuities. However, studies on variable thickness FGM plates using either closed-form solution or numerical methods are limited in number compared to constant thickness plates. As an example, a simple procedure was presented by Ait Atmane *et al.* (2011) where he studied the free vibration of sigmoid functionally graded beams with variable cross-section based on Bernoulli-Euler beam theory for simply supported, clamped and free ends type of supports. Rajasekaran and Wilson (2013), presented a numerical solution using finite difference method to evaluate the exact buckling loads and vibration frequencies of variable thickness isotropic plates. Various combinations of boundary conditions as well as many types of loading were considered. The researchers found a close agreement with the results in the literature. Mozafari (Mozafari and Ayob 2012, Mozafari *et al.* 2010a) studied the stability of a simply supported FGM plates with linearly varying thickness under mechanical buckling load using the higher-order theory assumptions. The presented formulation is based on Love-Kirchhoff hypothesis and the Sanders non-linear strain-displacement relations.

Few studies were carried out specifically for the thermal analysis of FGM plates with variable thickness. Mozafari *et al.* (2010b), based on the same assumptions mentioned previously, they studied the effect of thickness variation on the thermal buckling of FGM plates. Moreover, Mozafari *et al.* (2012a) used a colonial competitive algorithm for optimized critical thermal buckling load for a FGM plate with variable thickness. In another paper (2012b), they based their work on imperialist competitive algorithm to optimization of critical buckling temperature for FGM plates with a variable thickness under non-uniform temperature load using a third-order shear deformation; the objective of this study was to maximize the critical temperature capacity of a FGM plate. Ghomshei and Abbasi (2013) developed a finite element formulation for analyzing the axisymmetric thermal buckling of FGM annular plates with a variable thickness. Pouladvand (2009) examined thermal stability of thin FG rectangular plates with variable thickness, the plate

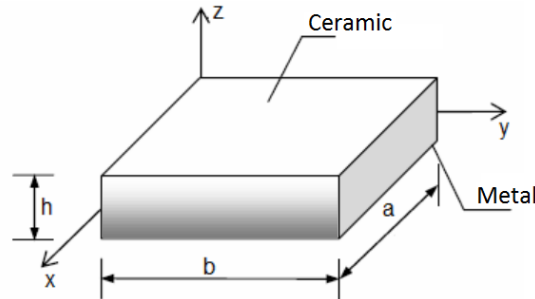


Fig. 1 Typical FGM plate

was considered simply supported in all edges, and the stability and equilibrium equation of plate was derived based on classical plate theory. The buckling analysis of FG plate was loaded under uniform, linear and non-linear temperature gradient through the thickness.

It is intended here to accurately determine the critical buckling temperature in functionally graded plates with constant as well as variable thickness under uniform temperature rise. To this end, based on an analytical formulation to evaluate the critical buckling temperature difference, the governing equation is obtained. This equation is solved for simply supported BCs using the finite difference method. It should be mentioned that the finite difference method is adopted in order to have the ability of including the plate thickness variation. The effects of material and geometric properties are studied.

## 2. Theoretical formulation

Consider an elastic rectangular plate. The local coordinates  $x$  and  $y$  define the mid-plan of the plate, whereas the  $z$ -axis originated at the middle surface of the plate is in the thickness direction, Fig. 1. The material properties, such as Young’s modulus on the upper and lower surfaces are different but are pre-assigned according to the performance demands.

The variation of FGM constituents follows a function where most researchers use the power-law function, exponential function, or sigmoid function to describe the material variation in terms of volume fractions. In order to compare the current study results with those of other researchers, two types of variations are used: Sigmoid (S-FGM) and power-law variations (P-FGM).

## 3. Estimation of mechanical properties of FGM

### 3.1 Sigmoid FGM variation

The sigmoid variation (S-FGM) can be described in terms of volume fraction as follows

$$\begin{aligned}
 V_f^1(z) &= 1 - \frac{1}{2} \left(1 - \frac{2z}{h}\right)^k & 0 \leq z \leq \frac{h}{2} \\
 V_f^2(z) &= \frac{1}{2} \left(1 + \frac{2z}{h}\right)^k & -\frac{h}{2} \leq z \leq 0
 \end{aligned}
 \tag{1}$$

where  $k$  is the material parameter that dictates the material variation profile through the thickness  $h$ .

By using the rule of mixture, the material properties such as modulus of elasticity  $E$  and thermal expansion  $\alpha$  are assumed to be function of the constituent materials as, Fig. 2(a)

$$E(z) = \begin{cases} V_f^1(z)E_c + (1 - V_f^1(z))E_m & 0 \leq z \leq \frac{h}{2} \\ V_f^2(z)E_c + (1 - V_f^2(z))E_m & -\frac{h}{2} \leq z \leq 0 \end{cases} \quad (2)$$

$$\alpha(z) = \begin{cases} V_f^1(z)\alpha_c + (1 - V_f^1(z))\alpha_m & 0 \leq z \leq \frac{h}{2} \\ V_f^2(z)\alpha_c + (1 - V_f^2(z))\alpha_m & -\frac{h}{2} \leq z \leq 0 \end{cases} \quad (3)$$

where the indices  $\alpha_c$  and  $\alpha_m$  indicate the property of the ceramic and metal of the FGM plate, respectively.

### 3.2 Power-law variation

For power-law type of material distribution (P-FGM), the volume fractions of ceramic  $V_c$  and metal  $V_m$  are given by

$$V_c = \left(\frac{z}{h} + \frac{1}{2}\right)^k, \quad k \geq 0 \quad (4a)$$

$$V_m(z) + V_c(z) = 1 \quad (4b)$$

The material properties of the FGM plate are expressed as follows, Fig. 2(b)

$$E(z) = E_c V_c + E_m (1 - V_c) \quad (5a)$$

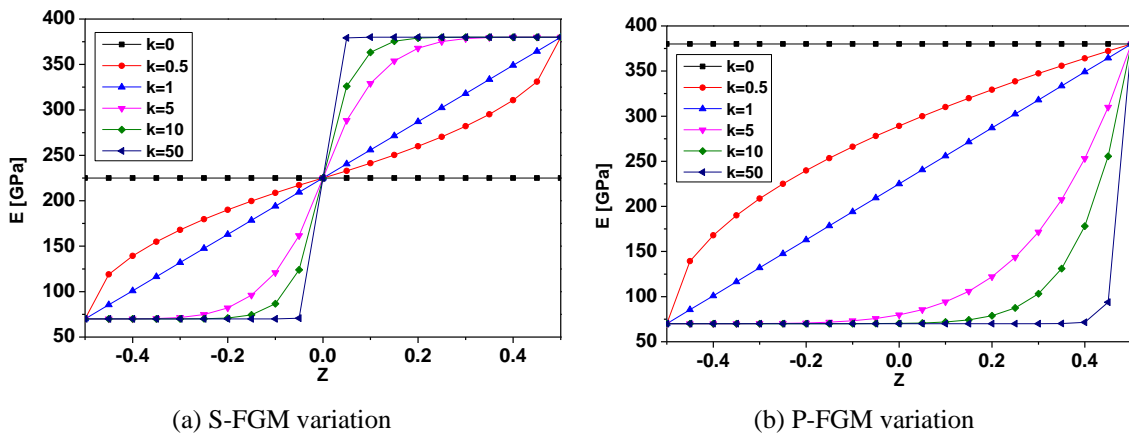


Fig. 2 Young's modulus variation in terms of the material parameter  $k$  for S-FGM and P-FGM plate

$$\alpha(z) = \alpha_c V_c + \alpha_m (1 - V_c) \tag{5b}$$

### 3.3 Formulation of the stability equations

Assuming the FGM plate shown in Fig. 1, with  $u, v, w$  denote the displacement of the neutral plane of the plate in  $x, y, z$  directions, respectively. The strains of the plate can be expressed according to the first order shear deformation theory as given in Eq. (6). Besides, the forces and moments per unit length are given in terms of the stress components through the thickness as Eq. (7)

$$\begin{aligned} \varepsilon_x &= u_{,x} + z \phi_{x,x} \\ \varepsilon_y &= v_{,y} + z \phi_{y,y} \\ \gamma_{xy} &= u_{,y} + v_{,x} + z (\phi_{x,y} + \phi_{y,x}) \\ \gamma_{xz} &= \phi_x + w_{,x} \\ \gamma_{yz} &= \phi_y + w_{,y} \end{aligned} \tag{6}$$

$$\begin{aligned} N_{ij} &= \int_{-h/2}^{h/2} \sigma_{ij} dz \\ M_{ij} &= \int_{-h/2}^{h/2} \sigma_{ij} z dz \\ Q_{ij} &= \int_{-h/2}^{h/2} \tau_{ij} dz \end{aligned} \tag{7}$$

The nonlinear equations of equilibrium according to Von Karman's tensor are given by

$$\begin{aligned} N_{x,x} + N_{xy,y} &= 0 \\ N_{y,y} + N_{xy,x} &= 0 \\ M_{x,x} + M_{xy,y} - Q_x &= 0 \\ M_{xy,x} + M_{y,y} - Q_y &= 0 \\ Q_{x,x} + Q_{y,y} + q + N_x w_{,xx} + N_y w_{,yy} + 2 N_{xy} w_{,xy} &= 0 \end{aligned} \tag{8}$$

The use of Eqs. (2)-(3), (6)-(7) reduces Eq. (8) to the following equation

$$\begin{aligned} \nabla^4 w + \frac{2(1+\nu)}{E_1} \nabla^2 (N_x w_{,xx} + N_y w_{,yy} + 2 N_{xy} w_{,xy} + q) \\ - \frac{E_1(1-\nu^2)}{E_1 E_3 - E_2^2} (N_x w_{,xx} + N_y w_{,yy} + 2 N_{xy} w_{,xy} + q) = 0 \end{aligned} \tag{9}$$

where

$$(E_1, E_2, E_3) = \int_{-h/2}^{h/2} (1, z, z^2) E(z) dz \tag{10}$$

The stability equations are established through using the critical equilibrium method. By assuming that the state of stable equilibrium of a general plate under thermal load may be simply

designated by the deflection  $w_0$ . The displacement of the neighboring state is given by

$$\Delta w = w_0 + w_1 \quad (11)$$

where  $w_1$  is an arbitrarily small increment of displacement. So, by substituting Eq. (11) into Eq. (9) and subtracting the original equation, results in the following stability equation

$$\begin{aligned} \nabla^4 w_1 + \frac{2(1+\nu)}{E_1} \nabla^2 (N_x^0 w_{1,xx} + N_y^0 w_{1,yy} + 2 N_{xy}^0 w_{1,xy}) \\ - \frac{E_1(1-\nu^2)}{E_1 E_3 - E_2^2} (N_x^0 w_{1,xx} + N_y^0 w_{1,yy} + 2 N_{xy}^0 w_{1,xy}) = 0 \end{aligned} \quad (12)$$

where,  $N_x^0, N_y^0$  and  $N_{xy}^0$  are the pre-buckling force resultants.

Once the pre-buckling thermal forces are found, the buckling temperature difference  $\Delta T_{cr}$  can be evaluated.

By solving the membrane form of equilibrium equations, this gives the pre-buckling force resultants

$$\begin{aligned} N_x^0 &= -\frac{\Phi}{1-\nu} \\ N_y^0 &= -\frac{\Phi}{1-\nu} \\ N_{xy}^0 &= 0 \end{aligned} \quad (13)$$

Assuming a uniform temperature rise and using Eq. (10), we have

$$\Phi = P \Delta T \quad (14)$$

where

$$P = \int_{-h/2}^{h/2} E(z) \alpha(z) dz \quad (15)$$

Substituting Eq. (13) and Eq. (14) into Eq. (12), one obtains

$$\nabla^4 w_1 - \frac{2(1+\nu)}{E_1} \frac{P \Delta T}{1-\nu} \nabla^4 w_1 + \frac{E_1(1-\nu^2)}{E_1 E_3 - E_2^2} \frac{P \Delta T}{1-\nu} \nabla^2 w_1 = 0 \quad (16)$$

The simply supported boundary conditions are defined as

$$\begin{aligned} w_1 &= 0 \\ M_{x1} &= 0 \quad \text{at } x = 0, a \\ \phi_{y1} &= 0 \end{aligned} \quad (17)$$

$$\begin{aligned} w_1 &= 0 \\ M_{y1} &= 0 \quad \text{at } y = 0, b \\ \phi_{x1} &= 0 \end{aligned} \quad (18)$$

### 4. Finite difference solution

The governing equation presented by Eq. (16) is a fourth order differential equation which can be solved using finite difference method. The objective of using finite difference method is to have extra capabilities such as including thickness variation, while including such capability in analytical procedure can usually lead to complex expressions that are difficult to be resolved.

To do so, we consider a rectangular FGM plate shown in Fig. 3 meshed into  $n \times m$  nodes spaced by  $\Delta h$  in  $x$  and  $y$  directions.

Eq. (16) is simplified as

$$\nabla^4 W \cdot A + \nabla^2 W \cdot B = 0 \tag{19}$$

where

$$W = w_1$$

$$A = 1 - \frac{2(1 + \nu) P \Delta T}{E_1 (1 - \nu)} \tag{20}$$

$$B = \frac{E_1 (1 - \nu^2) P \Delta T}{E_1 E_3 - E_2^2 (1 - \nu)}$$

Eq. (19) can be written at node  $(i, j)$  in finite difference (FD) format as follows

$$\begin{aligned} & \left( \frac{20A}{\Delta h^2} - 4B \right) \cdot W_{(i,j)} + \frac{A}{\Delta h^2} \cdot W_{(i,j-2)} + \left( -\frac{8A}{\Delta h^2} + B \right) \cdot W_{(i,j-1)} + \left( -\frac{8A}{\Delta h^2} + B \right) \cdot W_{(i,j+1)} \\ & + \frac{A}{\Delta h^2} \cdot W_{(i,j+2)} + \frac{A}{\Delta h^2} \cdot W_{(i-2,j)} + \left( -\frac{8A}{\Delta h^2} + B \right) \cdot W_{(i-1,j)} + \frac{2A}{\Delta h^2} \cdot W_{(i-1,j-1)} \\ & + \frac{2A}{\Delta h^2} \cdot W_{(i-1,j+1)} + \left( -\frac{8A}{\Delta h^2} + B \right) \cdot W_{(i+1,j)} + \frac{2A}{\Delta h^2} \cdot W_{(i+1,j-1)} + \frac{2A}{\Delta h^2} \cdot W_{(i+1,j+1)} \\ & + \frac{A}{\Delta h^2} \cdot W_{(i+2,j)} = 0 \end{aligned} \tag{21}$$

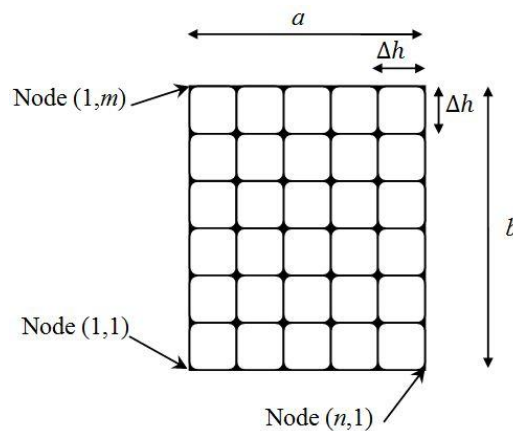


Fig. 3 Finite difference mesh of the plate

The mesh presented by Eq. (21) is applied at the nodes with coordinates  $(i = 2..n - 1, j = 2..m - 1)$ . Noting that this operation will result virtual nodes at the lines  $(i = 2, i = n - 1, j = 2, j = m - 1)$ . The virtual nodes can be eliminated using the following boundary conditions. Since the plate is simply supported, all the displacements along the edges equal to zero, i.e.,

$$W_{(i,j)} = 0 \quad \text{at} \quad [i = (1, n) \text{ and } j = (1..m)] \text{ and } [i = (1..n) \text{ and } j = (1, m)] \quad (22)$$

Also, the moment at all edges equals to zero ( $M = 0$ ), where the moment can be expressed in terms of deflection as

$$\frac{\partial^2 W}{\partial x^2} + \frac{\partial^2 W}{\partial y^2} = -\frac{M}{D} \quad (23)$$

As an illustrative example, at the bottom edge ( $j = 1$ ), the moment can be expressed in finite difference at each node  $(i, 1)$  as

$$\frac{1}{\Delta h^2} (-4W_{(i,1)} + W_{(i,0)} + W_{(i,2)} + W_{(i+1,1)} + W_{(i-1,1)}) = -\frac{M_{(i,1)}}{D_{(i,1)}} = 0 \quad (24)$$

Since all  $W_{(i,1)} = 0$  (1st boundary condition), the expression (24) can be simplified as

$$W_{(i,0)} = -W_{(i,2)} \quad (25)$$

Where  $W_{(i,0)}$  are virtual nodes to be substituted in Eq. (21) at nodes  $(i, j = 2)$ , one can get

$$\begin{aligned} & \left(\frac{19A}{\Delta h^2} - 4B\right) \cdot W_{(i,2)} + \left(-\frac{8A}{\Delta h^2} + B\right) \cdot W_{(i,1)} + \left(-\frac{8A}{\Delta h^2} + B\right) \cdot W_{(i,3)} + \frac{A}{\Delta h^2} \cdot W_{(i,4)} \\ & + \frac{A}{\Delta h^2} \cdot W_{(i-2,2)} + \left(-\frac{8A}{\Delta h^2} + B\right) \cdot W_{(i-1,2)} + \frac{2A}{\Delta h^2} \cdot W_{(i-1,1)} + \frac{2A}{\Delta h^2} \cdot W_{(i-1,3)} \\ & + \left(-\frac{8A}{\Delta h^2} + B\right) \cdot W_{(i+1,2)} + \frac{2A}{\Delta h^2} \cdot W_{(i+1,1)} + \frac{2A}{\Delta h^2} \cdot W_{(i+1,3)} + \frac{A}{\Delta h^2} \cdot W_{(i+2,2)} = 0 \end{aligned} \quad (26)$$

By applying the same principle for all other edges, all the virtual nodes can be eliminated. Finally, the following system of simultaneous equations is obtained

$$\begin{pmatrix} \left(\frac{18A}{\Delta h^2} - 4B\right) & -\frac{8A}{\Delta h^2} + B & \frac{A}{\Delta h^2} & \dots & \dots & \dots & \dots & \dots & 0 & 0 & 0 \\ -\frac{8A}{\Delta h^2} + B & \left(\frac{19A}{\Delta h^2} - 4B\right) & -\frac{8A}{\Delta h^2} + B & \dots & \dots & \dots & \dots & \dots & 0 & 0 & 0 \\ \frac{A}{\Delta h^2} & -\frac{8A}{\Delta h^2} + B & \left(\frac{20A}{\Delta h^2} - 4B\right) & \dots & \dots & \dots & \dots & \dots & 0 & 0 & 0 \\ \vdots & \vdots & \vdots & \ddots & \vdots & \vdots & \vdots & \vdots & 0 & 0 & 0 \\ \dots & \dots & \dots & \dots & \left(\frac{20A}{\Delta h^2} - 4B\right) & -\frac{8A}{\Delta h^2} + B & \frac{A}{\Delta h^2} & \dots & \dots & \dots & \dots \\ \dots & \dots & \dots & \dots & -\frac{8A}{\Delta h^2} + B & \left(\frac{20A}{\Delta h^2} - 4B\right) & -\frac{8A}{\Delta h^2} + B & \dots & \dots & \dots & \dots \\ \dots & \dots & \dots & \dots & \frac{A}{\Delta h^2} & -\frac{8A}{\Delta h^2} + B & \left(\frac{20A}{\Delta h^2} - 4B\right) & \dots & \dots & \dots & \dots \\ \dots & \dots & \dots & \dots & \vdots & \vdots & \vdots & \ddots & \vdots & \vdots & \vdots \\ 0 & 0 & 0 & \dots & \dots & \dots & \dots & \dots & \left(\frac{20A}{\Delta h^2} - 4B\right) & -\frac{8A}{\Delta h^2} + B & \frac{A}{\Delta h^2} \\ 0 & 0 & 0 & \dots & \dots & \dots & \dots & \dots & -\frac{8A}{\Delta h^2} + B & \left(\frac{19A}{\Delta h^2} - 4B\right) & -\frac{8A}{\Delta h^2} + B \\ 0 & 0 & 0 & \dots & \dots & \dots & \dots & \dots & \frac{A}{\Delta h^2} & -\frac{8A}{\Delta h^2} + B & \left(\frac{18A}{\Delta h^2} - 4B\right) \\ 0 & 0 & 0 & \dots \end{pmatrix} \begin{pmatrix} W_{(2,2)} \\ W_{(3,2)} \\ W_{(4,2)} \\ \vdots \\ W_{(i-1,j)} \\ W_{(i,j)} \\ W_{(i+1,j)} \\ \vdots \\ W_{(n-3,m-1)} \\ W_{(n-2,m-1)} \\ W_{(n-1,m-1)} \end{pmatrix} = \begin{pmatrix} 0 \\ 0 \\ 0 \\ \vdots \\ 0 \\ 0 \\ 0 \\ \vdots \\ 0 \\ 0 \\ 0 \end{pmatrix} \quad (27)$$

Solving the above homogeneous simultaneous equations system will result  $(n - 2) \times (m - 2)$  mode shapes for  $W_{(i,j)}$ . Then, to evaluate the critical temperature  $\Delta T_{cr}$ , the significant mode shape i.e., the first mode has to be used into Eq. (19).

However, to solve the Eq. (27), the value of  $\Delta T_{cr}$  which is incorporated in the values of  $A$  and  $B$ , must be known first. Hence, two strategies can be used:

- It is possible to use the trial and error technique to find the correct  $\Delta T_{cr}$ . Since the shape of the buckling mode  $W(x, y)$  is totally independent from the value  $\Delta T_{cr}$ , any initial value of  $\Delta T_{cr}$  to solve Eq. (27) found to have no effect on results of  $W_{(i,j)}$ .
- Otherwise, in the analytical solution of buckling analysis, the mode shapes  $W(x, y)$  are usually assumed to be sinusoidal function that satisfies the boundary conditions. Accordingly, to solve numerically the buckling or vibration of plates, it is then possible to assume that the shape modes are the same as given by  $\nabla^4 W(x, y) = 0$  since it has the same solution as assumed in the analytical solution.

The adopted technique to solve Eq. (27) the trial and error technique with assuming  $\Delta T_{cr} = 0$  as an initial value. Thus, Eq. (27) is arranged to the following expression

$$\begin{bmatrix}
 \left(\frac{18}{\Delta h^2}\right) & -\frac{8}{\Delta h^2} & \frac{1}{\Delta h^2} & \dots & \cdot & \cdot & \cdot & \cdot & 0 & 0 & 0 \\
 \frac{8}{\Delta h^2} & \left(\frac{19}{\Delta h^2}\right) & -\frac{8}{\Delta h^2} & \dots & \cdot & \cdot & \cdot & \cdot & 0 & 0 & 0 \\
 \frac{1}{\Delta h^2} & -\frac{8}{\Delta h^2} & \left(\frac{20}{\Delta h^2}\right) & \dots & \cdot & \cdot & \cdot & \cdot & 0 & 0 & 0 \\
 \vdots & \vdots & \vdots & \ddots & \vdots & \vdots & \vdots & \vdots & 0 & 0 & 0 \\
 \cdot & \cdot & \cdot & \dots & \left(\frac{20}{\Delta h^2}\right) & -\frac{8}{\Delta h^2} & \frac{1}{\Delta h^2} & \dots & \cdot & \cdot & \cdot \\
 \cdot & \cdot & \cdot & \dots & -\frac{8}{\Delta h^2} & \left(\frac{20}{\Delta h^2}\right) & -\frac{8}{\Delta h^2} & \dots & \cdot & \cdot & \cdot \\
 \cdot & \cdot & \cdot & \dots & \frac{1}{\Delta h^2} & -\frac{8}{\Delta h^2} & \left(\frac{20}{\Delta h^2}\right) & \dots & \cdot & \cdot & \cdot \\
 0 & 0 & 0 & \cdot & \vdots & \vdots & \vdots & \ddots & \cdot & \cdot & \cdot \\
 0 & 0 & 0 & \cdot & \cdot & \cdot & \cdot & \dots & \left(\frac{20}{\Delta h^2}\right) & -\frac{8}{\Delta h^2} & \frac{1}{\Delta h^2} \\
 0 & 0 & 0 & \cdot & \cdot & \cdot & \cdot & \dots & -\frac{8}{\Delta h^2} & \left(\frac{19}{\Delta h^2}\right) & -\frac{8}{\Delta h^2} \\
 0 & 0 & 0 & \cdot & \cdot & \cdot & \cdot & \dots & \frac{1}{\Delta h^2} & -\frac{8}{\Delta h^2} & \left(\frac{18}{\Delta h^2}\right)
 \end{bmatrix}
 \begin{Bmatrix}
 W_{(2,2)} \\
 W_{(3,2)} \\
 W_{(4,2)} \\
 \vdots \\
 W_{(i-1,j)} \\
 W_{(i,j)} \\
 W_{(i+1,j)} \\
 \vdots \\
 W_{(n-3,m-1)} \\
 W_{(n-2,m-1)} \\
 W_{(n-1,m-1)}
 \end{Bmatrix}
 =
 \begin{Bmatrix}
 0 \\
 0 \\
 0 \\
 \vdots \\
 0 \\
 0 \\
 0 \\
 \vdots \\
 0 \\
 0 \\
 0
 \end{Bmatrix}
 \quad (28)$$

By substituting the first mode vector  $W$  in Eq. (19) yields

$$\Delta T_{cr} = \frac{\nabla^4 W}{\frac{2(1 + \nu)P}{E_1(1 - \nu)} \nabla^4 W - \frac{E_1(1 - \nu^2)P}{(E_1 E_3 - E_2^2)(1 - \nu)} \nabla^2 W} \quad (29)$$

The Eq. (29) can be expressed in finite difference format at each node as given by eq. (30), while the adopted value of  $\Delta T_{cr}$  is the minimum value of  $\Delta T_{cr(i)}$

$$\Delta T_{cr(i)} = \frac{\left( \frac{20}{\Delta h^2} \cdot W_{(i,j)} - \frac{8}{\Delta h^2} \cdot W_{(i-1,j)} - \frac{8}{\Delta h^2} \cdot W_{(i+1,j)} - \frac{8}{\Delta h^2} \cdot W_{(i,j-1)} - \frac{8}{\Delta h^2} \cdot W_{(i,j+1)} \right. \\ \left. + \frac{2}{\Delta h^2} \cdot W_{(i-1,j-1)} + \frac{2}{\Delta h^2} \cdot W_{(i+1,j-1)} + \frac{2}{\Delta h^2} \cdot W_{(i-1,j+1)} + \frac{2}{\Delta h^2} \cdot W_{(i+1,j+1)} \right. \\ \left. + \frac{1}{\Delta h^2} \cdot W_{(i-2,j)} + \frac{1}{\Delta h^2} \cdot W_{(i+2,j)} + \frac{1}{\Delta h^2} \cdot W_{(i,j-2)} + \frac{1}{\Delta h^2} \cdot W_{(i,j+2)} \right)}{\left( \left( \frac{20C}{\Delta h^2} - 4D \right) \cdot W_{(i,j)} + \left( -\frac{8C}{\Delta h^2} + D \right) \cdot W_{(i-1,j)} + \left( -\frac{8C}{\Delta h^2} + D \right) \cdot W_{(i+1,j)} + \left( -\frac{8C}{\Delta h^2} + D \right) \cdot W_{(i,j-1)} \right) \\ \left( -\frac{8C}{\Delta h^2} + D \right) W_{(i,j+1)} + \frac{2C}{\Delta h^2} \cdot W_{(i-1,j-1)} + \frac{2C}{\Delta h^2} \cdot W_{(i+1,j-1)} + \frac{2C}{\Delta h^2} \cdot W_{(i-1,j+1)} + \frac{2C}{\Delta h^2} \cdot W_{(i+1,j+1)} \\ + \frac{C}{\Delta h^2} \cdot W_{(i-2,j)} + \frac{C}{\Delta h^2} \cdot W_{(i+2,j)} + \frac{C}{\Delta h^2} \cdot W_{(i,j-2)} + \frac{C}{\Delta h^2} \cdot W_{(i,j+2)} \right)} \quad (30)$$

where

$$C = \frac{2(1 + \nu)P}{E_1(1 - \nu)} \quad (31)$$

$$D = -\frac{E_1(1 - \nu^2)P}{(E_1E_3 - E_2^2)(1 - \nu)}$$

## 5. Thermal buckling analysis and results

### 5.1 Constant thickness FGM plate

A thermal buckling analysis of simply supported rectangular FGM plate with constant thickness has been carried out to validate the finite difference solution by comparing the results with the exact solution presented by Bouazza *et al.* (2009). The plate dimensions in  $x - y$  plane are  $a$  by  $b$  with  $a \leq b$ . The plate thickness is  $h$ , as shown in Fig. 1. The plate is assumed to have a sigmoid type of material distribution, as described by Eq. (1), and exposed to a uniform thermal load. The reference temperature is assumed to be  $5^\circ\text{C}$ . The metal and ceramic used in the FGM are Aluminum and Alumina with the following properties:  $E_m = 70 \text{ GPa}$ ,  $\alpha_m = 23 \times 10^{-6} (1/\text{C}^\circ)$  for the Aluminum and  $E_c = 380 \text{ GPa}$ ,  $\alpha_c = 7.4 \times 10^{-6} (1/\text{C}^\circ)$  for the Alumina. While, the Poisson's ratio  $\nu$  is assumed to be constant through the thickness.

As a first step, a convergence study of the finite difference formulation has been performed to examine the sensitivity of the analysis to the mesh density. According to Fig. 4 which represents the convergence rate of the FD solution, it was found that when the mesh density  $a/\Delta h$  (number of divisions) increases, the solution converges to the exact value given by Bouazza *et al.* (2009). In other words, the relative error of the results becomes smaller than 0.035% when the plate is divided into more than 40 segments each side. It should be also noted that, the finite difference solution errors for coarse mesh ( $a/\Delta h < 30$ ) are quite bigger for thin plate ( $a/h = 50$ ) than that of thick plate ( $a/h = 5$ ). However, for finest mesh used ( $a/\Delta h = 50$ ) the solution errors decrease to less than 0.035% and 0.017% for  $k = 0$  and  $k = 50$  respectively. Besides, it was remarked that the finer the mesh used, the longer time is required to resolve the problem, bearing in mind that in case of  $a/\Delta h = 50$ , there are 2601 nodes in the model.

Accordingly, the adopted mesh density for the rest of analysis was taken as  $a/\Delta h = 50$  which was found to be suitable and satisfactory in terms of accuracy and time consuming.

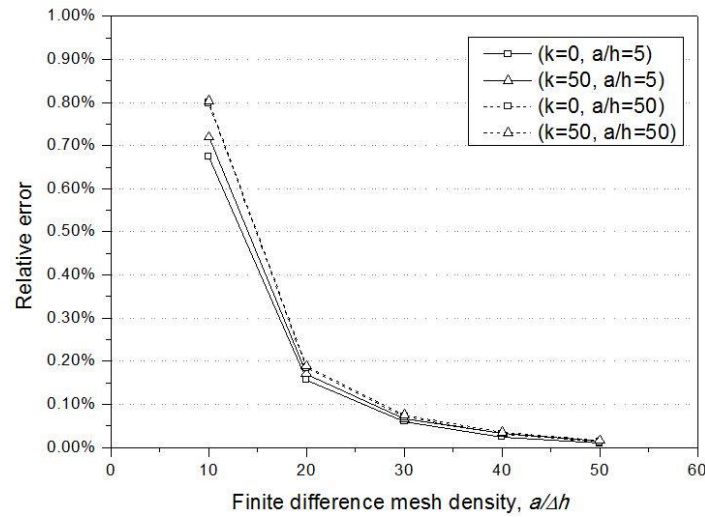


Fig. 4 Finite difference solution convergence

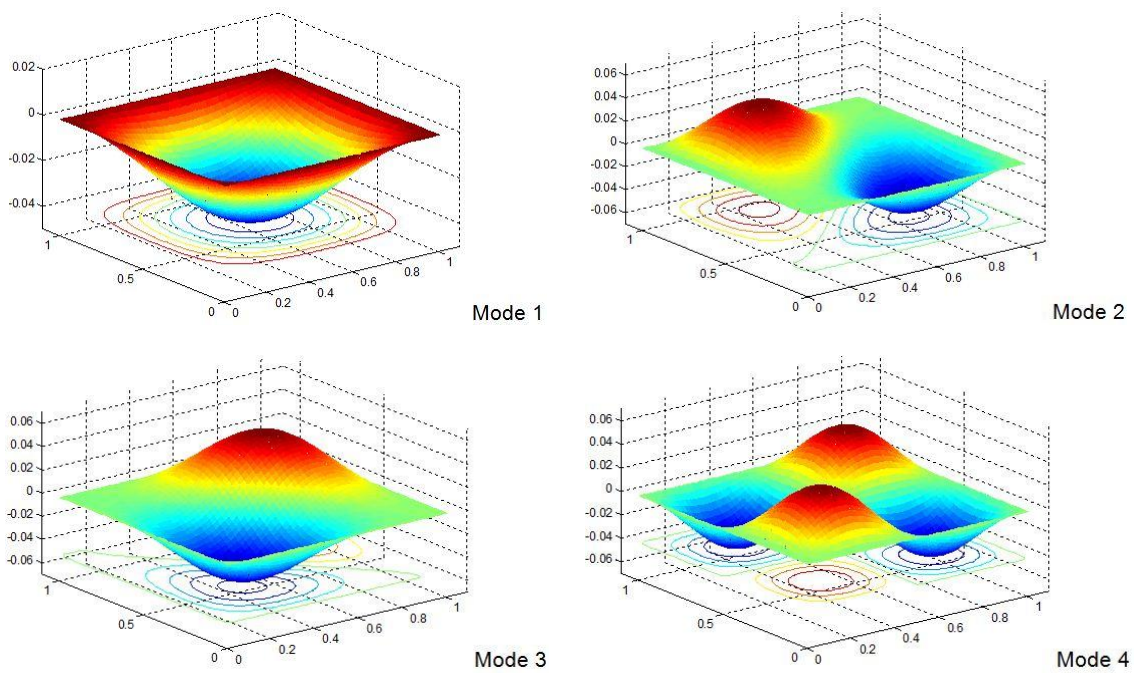


Fig. 5 Displacement  $W_{i,j}$  of the FGM plate under the first four natural modes

Table 1, represents a comparison between the exact solution presented by Bouazza *et al.* (2009) and the present finite difference solution for different ratios of  $a/h$  and  $b/a$  and different values of material parameter  $k$ . Fig. 5 represents the first four modes of the displacement  $W_{i,j}$  for FGM plate with  $b/a = 1$ ,  $a/h = 10$  and  $k = 10$ .

Table 1 Present finite difference solution vs. exact solution

$a/h$	Exact solution [Bouazza]	Finite difference mesh density ( $a/\Delta h$ )										
		10		20		30		40		50		
		$\Delta T_{cr}$	%error*	$\Delta T_{cr}$	% error*							
$k=0$	5	2802.902	2784.000	0.674%	2798.500	0.157%	2801.200	0.061%	2802.200	0.025%	2802.600	0.011%
	10	794.731	789.012	0.720%	793.680	0.132%	794.547	0.023%	794.850	0.015%	794.991	0.033%
	20	205.601	204.071	0.744%	205.320	0.137%	205.552	0.024%	205.633	0.016%	205.671	0.034%
	50	33.236	32.970	0.798%	33.174	0.185%	33.212	0.071%	33.225	0.031%	33.232	0.013%
$k=1$	5	2743.361	2724.400	0.691%	2739.000	0.159%	2741.700	0.061%	2742.600	0.028%	2743.000	0.013%
	10	764.145	758.256	0.771%	762.774	0.179%	763.613	0.070%	763.907	0.031%	764.043	0.013%
	20	196.649	195.090	0.793%	196.286	0.185%	196.508	0.072%	196.586	0.032%	196.622	0.014%
	50	31.725	31.471	0.800%	31.666	0.186%	31.702	0.072%	31.715	0.032%	31.720	0.014%
$k=10$	5	2797.583	2777.700	0.711%	2793.000	0.164%	2795.900	0.060%	2796.900	0.024%	2797.300	0.010%
	10	762.036	756.146	0.773%	760.690	0.177%	761.534	0.066%	761.829	0.027%	761.966	0.009%
	20	194.872	193.332	0.791%	194.520	0.181%	194.741	0.068%	194.818	0.028%	194.854	0.009%
	50	31.381	31.131	0.796%	31.324	0.182%	31.360	0.068%	31.372	0.028%	31.378	0.010%
$k=50$	5	2914.566	2893.600	0.719%	2909.600	0.170%	2912.600	0.067%	2913.600	0.033%	2914.100	0.016%
	10	792.918	786.729	0.781%	791.459	0.184%	792.337	0.073%	792.645	0.034%	792.787	0.017%
	20	202.700	201.083	0.798%	202.319	0.188%	202.548	0.075%	202.629	0.035%	202.666	0.017%
	50	32.638	32.376	0.803%	32.576	0.189%	32.614	0.075%	32.627	0.035%	32.633	0.017%

\*  $Relative\ error = \frac{Finite\ difference - Exact\ solution}{Exact\ solution} \%$ ; where the exact solution is given by Bouazza *et al.* (2009)

Based on Table 1, a very good agreement was found between the numerical and the analytical solution for different ranges of geometric and material properties. Thus, the present finite difference solution can be used efficiently to analyze buckling of FGM plate with a very good accuracy.

Generally, the results indicate that as the rigidity of the plate increases, the critical temperature increases. Noting that the plate rigidity increases when using lower values of  $a/h$ , and lower value of material parameter  $k$ . Also, the results indicate that the critical buckling temperature of FGM plates  $k \geq 1$  is lower than that of homogenous plate ( $k = 0$ ).

### 5.2 Thermal buckling of FGM plate with linear thickness variation

The finite difference procedure described above has been extended to be used for evaluating the thermal buckling of FGM plate with variable thickness. The thickness variation capability can be easily included in the FD formulation by varying the thickness at each node, i.e., introducing a variable thickness  $h_{i,j}$  which represents the plate thickness at the node  $(i,j)$ , as clarified in Fig. 6.

Two types of linear thickness variation have been studied, linear variation in one direction and linear variation in both directions. The linear variation of the plate thickness in  $x$  or  $y$ -direction is assumed to change according to the following equation

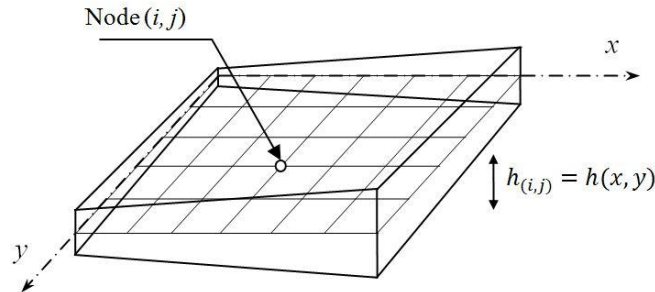


Fig. 6 FGM plate with linear variable thickness

$$\begin{aligned}
 h(x) &= c_1 x + c_2 \\
 h(y) &= c_1 y + c_2
 \end{aligned}
 \tag{32}$$

Where,  $c_1$  is a non-dimensional parameter which represents the slope of the variation, and  $c_2$  is nominal thickness of the plate at origin. While, in case of linear variation in both  $x$  and  $y$  directions, the following equation is used

$$h(x, y) = c_1 x + c_1 y + c_2
 \tag{33}$$

The example of FGM plate with variable thickness which was analyzed by Pouladvand (2009) has been adopted to be used for the comparison. The FGM plate constituents follow a power-law type of distribution as described previously by Eqs. (4a), (4b), (5a) and (5b). The top surface of the plate is ceramic-rich while the bottom surface is metal-rich. The ceramic and metal properties are varied as described by Eq. (5).

Figs. 7, 8, 9 and 10 present the thermal buckling of FGM plates with linear thickness variation predicted by the present finite difference solution against the closed-form solution presented by Pouladvand (2009).

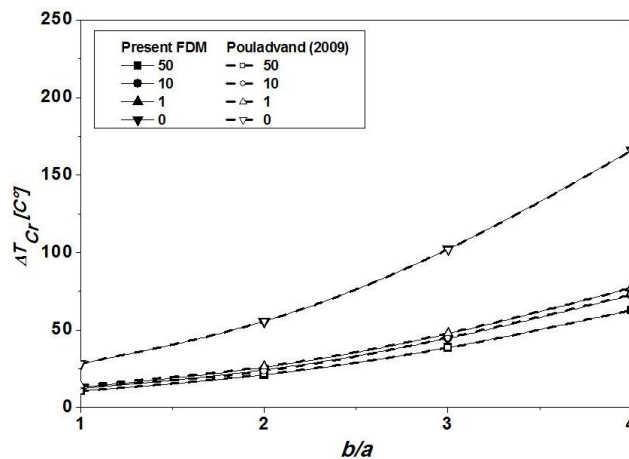


Fig. 7 Effect of the aspect ratio on the buckling critical temperature in the plate with variable thickness in  $x$ -direction

As an overview, and based on Figs. 7, 8, 9 and 10, one can observe that the present numerical solution results methods are close to the exact solution. It should be mentioned that the solution presented by Pouladvand (2009) is also based on the classical plate theory (CPT). Accordingly, the later comparison validates and confirms that the finite difference method is accurate, efficient, and relatively simple for predicting the thermal buckling behaviour of FGM plates with linear thickness variation.

Moreover, the simplicity to introduce the thickness variation in finite difference solution, permit us to accurately analyze FGM plates with any type of thickness variation such parabolic or sinusoidal variation. While, varying the plate thickness in the analytical solutions leads usually to complex expressions that are difficult or impossible to be solved.

Figs. 7 and 8 show the effect of the aspect ratio  $b/a$  and the material distribution parameter  $k$  on the critical buckling temperature difference  $\Delta T_{cr}$  of FGM plate linear variable thickness in

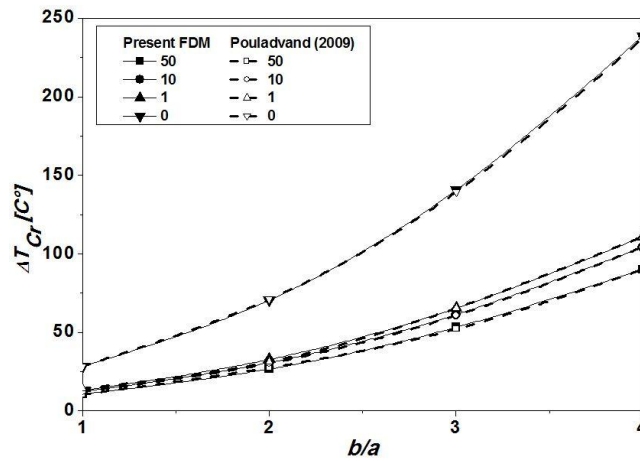


Fig. 8 Effect of the aspect ratio on the buckling critical temperature in the plate with variable thickness in y-direction

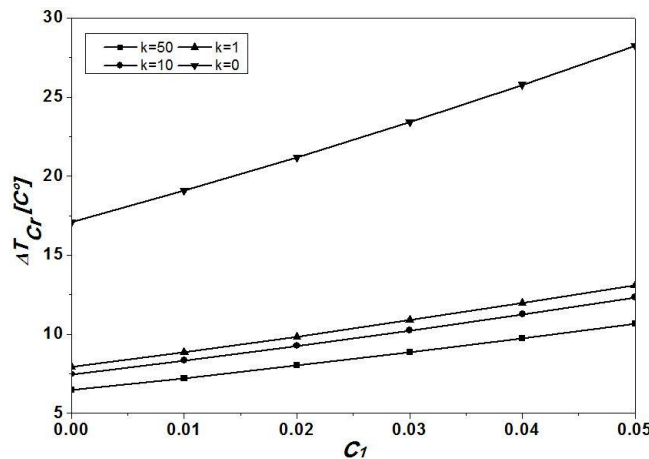


Fig. 9 The buckling critical temperature in terms of  $c_1$  for square plate with variable thickness in x-direction,  $c_2 = 0.01a$

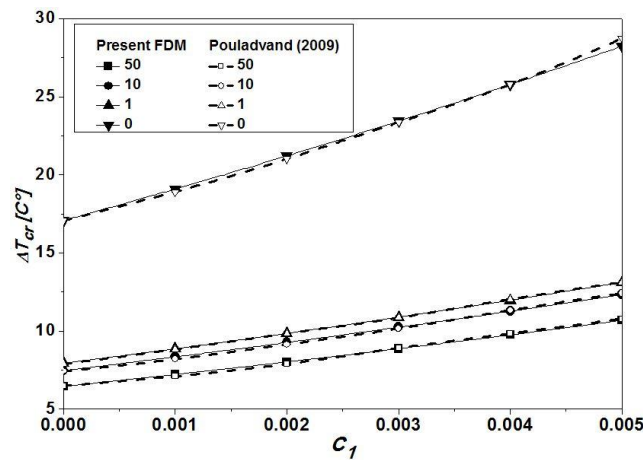


Fig. 10 The buckling critical temperature in terms of  $c_1$  for square plate with variable thickness in  $x$  and  $y$ -direction,  $c_2 = 0.01a$

$x$ -direction, and  $y$ -direction, respectively. The linear thickness parameters of the plate in the two figures have the values of  $c_1 = 0.005, c_2 = 0.01a$ .

By comparing the effect of the linear thickness variation in  $x$ -direction and  $y$ -direction on the critical temperature difference  $\Delta T_{cr}$ , one can observe that  $\Delta T_{cr}$  in  $x$ -direction is lower than that of  $y$ -direction for all geometric and material parameters. This indicates that FGM plates with linear variable thickness in  $y$ -direction have a higher thermal buckling resistance than FGM plates with linear thickness variation in  $x$ -direction.

The effect of thickness variation parameters  $c_1$  on the critical temperature difference  $\Delta T_{cr}$ , for different material distribution parameter  $k$ , is illustrated in Fig. 9. The results indicate that the thermal buckling resistance of the plate increases when  $c_1$  increases, but with a low sensitivity to different material parameters  $k$  compared to a homogenous plate ( $k = 0$ ).

In this section, the FGM plate is square and has a linear variable thickness in both  $x$  and  $y$ -directions. The effect of the thickness variation parameter  $c_1$  on the critical temperature difference  $\Delta T_{cr}$  for difference values of material parameter  $k$ , is presented by Fig. 10. The results confirm also that increasing the thickness variation parameter  $c_1$  leads to an increase in the thermal buckling resistance of the plate. However, this increase is not highly affected by the material distribution parameter  $k$  compared to a homogenous plate.

## 6. Conclusions

This study deals with the thermal buckling analysis of FGM plates having linear thickness variation. The solution is based on an analytical procedure for constant thickness FGM plate, then the finite difference method is used to introduce the variable thickness. The results for of constant thickness plate as well as variable thickness are compared with those found in the literature.

According to the obtained results, it was found that the present numerical method was very close to the analytical solution found in the literature for plate with constant thickness as well as linear variable thickness. Therefore, the finite difference method was judged to be an accurate tool

and relatively easy method to evaluate the thermal buckling of FGM plates.

Moreover, the parametric study indicates that the thermal resistance of the FGM plates increases with the increase of its rigidity. The latter is directly related to the values of  $a/h$ ,  $b/a$ , the material distribution parameter  $k$ , and the thickness parameter  $c_1$  in case of linear FGM plates. Also, the increase of the thickness variation parameter leads to an increase in the thermal buckling resistance of the plate. However, this increase is slightly affected by the material distribution parameter compared to a homogenous plate.

## References

- Ait Atmane, H., Tounsi, A., Ziane, N. and Mechab, I. (2011), "Mathematical solution for free vibration of sigmoid functionally graded beams with varying cross-section", *Steel Compos. Struct., Int. J.*, **11**(6), 489-504.
- Bouazza, M., Tounsi, A., Bedia Adda, E.A. and Megueni, A. (2009), "Buckling analysis of functionally graded plates with simply supported edges", *Leonardo J. Sci.*, **8**(15), 21-32.
- Fekrar, A., Zidi, M., Boumia, L., Ait Atmane, H., Tounsi, A. and Bedia Adda, E.A. (2013), "Thermal buckling of AL/AL<sub>2</sub>O<sub>3</sub> functionally graded plates based on first order theory", *Nature Technol. J. A-Fundamental & Eng. Sci.*, **A**(08), 12-16.
- Ghomshei, M.M. and Abbasi, V. (2013), "Thermal buckling analysis of annular FGM plate having variable thickness under thermal load of arbitrary distribution by finite element method", *J. Mech. Sci. Tech.*, **27**(4), 1031-1039.
- Hiroyuki, M. (2009), "Stress analysis of functionally graded plates subjected to thermal and mechanical loadings", *Compos. Struct.*, **87**(4), 344-357.
- Javaheri, R. and Eslami, M.R. (2002a), "Buckling of functionally graded plates under in-plane compressive loading", *ZAMM Z Angew. Mater. Mech.*, **82**(4), 277-283.
- Javaheri, R. and Eslami, M.R. (2002b), "Thermal buckling of functionally graded plates", *AIAA. J.*, **40**(1), 162-169.
- Javaheri, R. and Eslami, M.R. (2002c), "Thermal buckling of functionally graded plates based on higher order theory", *J. Therm. Stress.*, **25**(1), 603-625.
- Koohkan, H., Kimiaefar, A., Mansourabadi, A. and Vaghefi, R. (2010), "An analytical approach on the buckling analysis of circular, solid and annular functionally graded thin plates", *J. Mech. Eng.*, **41**(1), 7-14.
- Lanhe, W. (2004), "Thermal buckling of a simply supported moderately thick rectangular FGM plate", *Compos. Struct.*, **64**(2), 211-218.
- Mohammadi, M., Saidi, A.R. and Jomehzadeh, E. (2010), "Levy solution for buckling analysis of functionally graded rectangular plates", *Appl. Compos. Mater.*, **17**(1), 81-93.
- Mozafari, H. and Ayob, A. (2012), "Effect of thickness variation on the mechanical buckling load in plates made of functionally graded materials", *Procedia Technology*, **1**(2012), 496-504.
- Mozafari, H., Ayob, A. and Alias, A. (2010a), "Influence of thickness variation on the buckling load in plates made of functionally graded materials", *Eur. J. Sci. Res.*, **47**(3), 422-435.
- Mozafari, H., Ayob, A. and Alias, A. (2010b), "Verification of the thermal buckling load in plates made of functionally graded materials", *Int. J. Eng.*, **4**(5), 338-356.
- Mozafari, H., Abdi, B. and Ayob, A. (2012a-b), "Optimization of temperature-dependent functionally graded material based on colonial competitive algorithm", *Appl. Mech. Mater.*, **121-126**, 4575-4580.
- Mozafari, H., Abdi, B., Ayob, A. and Alias, A. (2012b-c), "Optimum critical buckling of functionally graded plates under non-linear temperature by using imperialist competitive algorithm", *Appl. Mech. Mater.*, **110-116**, 3429-3433.
- Noseir, A. and Reddy, J.N. (1992), "On vibration and buckling of symmetric laminated plates according to shear deformation theories", *Acta. Mech.*, **94**(3-4), 145-169.

- Pouladvand, M. (2009), "Thermal stability of thin rectangular plates with variable thickness made of functionally graded material", *J Solid Mech.*, **1**(3), 171-189.
- Praveen, G.N. and Reddy, J.N. (1998), "Nonlinear transient thermoelastic analysis of functionally graded ceramic-metal plates", *Int. J. Solid. Struct.*, **35**(33), 4457-4476.
- Rajasekaran, S. and Wilson, J.A. (2013), "Buckling and vibration of rectangular plates of variable thickness with different end conditions by finite difference technique", *Struct. Eng. Mech., Int. J.*, **46**(2), 269-294.
- Raki, M., Alipour, R. and Kamanbedast, A. (2012), "Thermal buckling of thin rectangular FGM plate", *World Appl. Sci. J.*, **16**(1), 52-62.
- Rohit, S. and Maiti, P.R. (2012), "Buckling of simply supported FGM plates under uniaxial load", *Int. J. Civil Struct. Eng.*, **2**(4), 1035-1050.
- Zenkour, A.M. and Mashat, D.S. (2010), "Thermal buckling analysis of ceramic-metal functionally graded plates", *Natural Sci.*, **2**(9), 968-978.

CC